

## Supplementary Material

**Supplementary Table S1:** Strains and plasmids constructed and used in the present study.

Designation	Size (kb)	Description
pGT1803	4.2	pGEMT containing a 1.2-kb fragment, the coding sequence of <i>slr1803</i> amplified by PCR
pGT1803Km-	5.3	pGT1803 containing a partial deleted <i>slr1803</i> ( <i>aphII</i> gene inserted after deletion of the internal <i>HincII</i> fragment opposite to the transcription direction of <i>slr1803</i> )
p1803pBADHISB	5.0	pBADHISB containing a 0.9-kb fragment, the coding sequence of <i>slr1803</i> amplified by PCR
pGT0729	4.8	pGEMT containing a 1.8-kb fragment, the coding sequence of <i>sll0729</i> amplified by PCR
pGT0729ΔKm	5.6	pGT0729 containing a partial deleted <i>sll0729</i> ( <i>aphII</i> gene inserted after deletion of the internal <i>EcoRI/BclI</i> fragment opposite to the transcription direction of <i>sll0729</i> )
p0729pBADHISC	5.0	pBADHISC containing a 0.9-kb fragment, the coding sequence of <i>sll0729</i> amplified by PCR
pVZ322-P <sub>ziaA</sub> :: <i>sll0729</i>	8.6	Self-replicating pVZ322 plasmid carrying the <i>sll0729</i> gene in fusion with the promoter of the <i>ziaA</i> gene of <i>Synechocystis</i> , the used promoter sequence covers the range between genome pos. 3060796 and 3061359 (in Genbank file BA000022) and also includes the <i>ziaR</i> gene encoding the transcriptional regulator of <i>ziaA</i>
pVZ322-P <sub>ziaA</sub> :: <i>ssl1378</i>	8.0	Self-replicating pVZ322 plasmid carrying the <i>ssl1378</i> gene in fusion with the promoter of the <i>ziaA</i> gene of <i>Synechocystis</i>
pGT6095	4.4	pGEMT containing a 1.4-kb fragment, the coding sequence of <i>slr6095</i> amplified by PCR
pGT6095Km-	5.7	pGT6095 containing an <i>aphII</i> gene inserted opposite to the transcription direction of <i>slr6095</i>
pGT8009	5.8	pGEMT containing a 2.6-kb fragment, the coding sequence of <i>sll8009</i> amplified by PCR

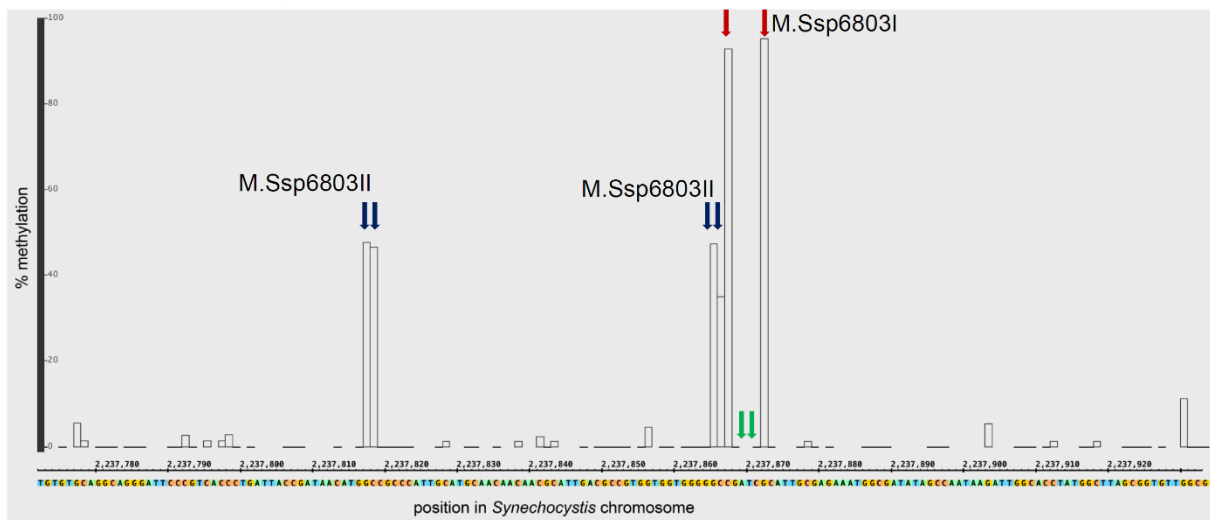
pGT8009ΔKm	6.0	pGT8009 containing a partial deleted <i>sll8009</i> ( <i>aphII</i> gene inserted after deletion of the internal <i>NheI/NheI</i> fragment opposite to the transcription direction of <i>sll8009</i> )
pGT6050	7.3	pGEMT containing a 3.3-kb fragment, the coding sequence of <i>slr6050</i> amplified by PCR
pGT6050ΔKm	7.6	pGT6050 containing a partial deleted <i>slr6050</i> ( <i>aphII</i> gene inserted after deletion of the internal <i>ClaI/ClaI</i> fragment opposite to the transcription direction of <i>slr6050</i> )
Δ <i>slr1803</i>		<i>Synechocystis</i> mutant obtained after transformation of the wild type with pGT1803Km-
Δ <i>sll0729</i>		<i>Synechocystis</i> mutant obtained after transformation of the wild type with pGT0729Km-
Δ <i>slr0214</i>		<i>Synechocystis</i> mutant with interrupted gene <i>slr0214</i> for MSsp6803I [18]
Δ <i>slr6095</i>		<i>Synechocystis</i> mutant obtained after transformation of the wild type with pGT6095Km-
Δ <i>sll8009</i>		<i>Synechocystis</i> mutant obtained after transformation of the wild type with pGT8009ΔKm
Δ <i>slr6050</i>		<i>Synechocystis</i> mutant obtained after transformation of the wild type with pGT6050ΔKm
Δ <i>sll0729</i> + <i>sll0729</i>		<i>Synechocystis</i> Δ <i>sll0729</i> strain harbouring the pVZ322-PziaA :: <i>sll0729</i>
Δ <i>ssl1378</i> + <i>ssl1378</i>		<i>Synechocystis</i> Δ <i>sll0729</i> strain harbouring the pVZ322-PziaA :: <i>ssl1378</i>

**Supplementary Table S2: Primers used in the present study.**

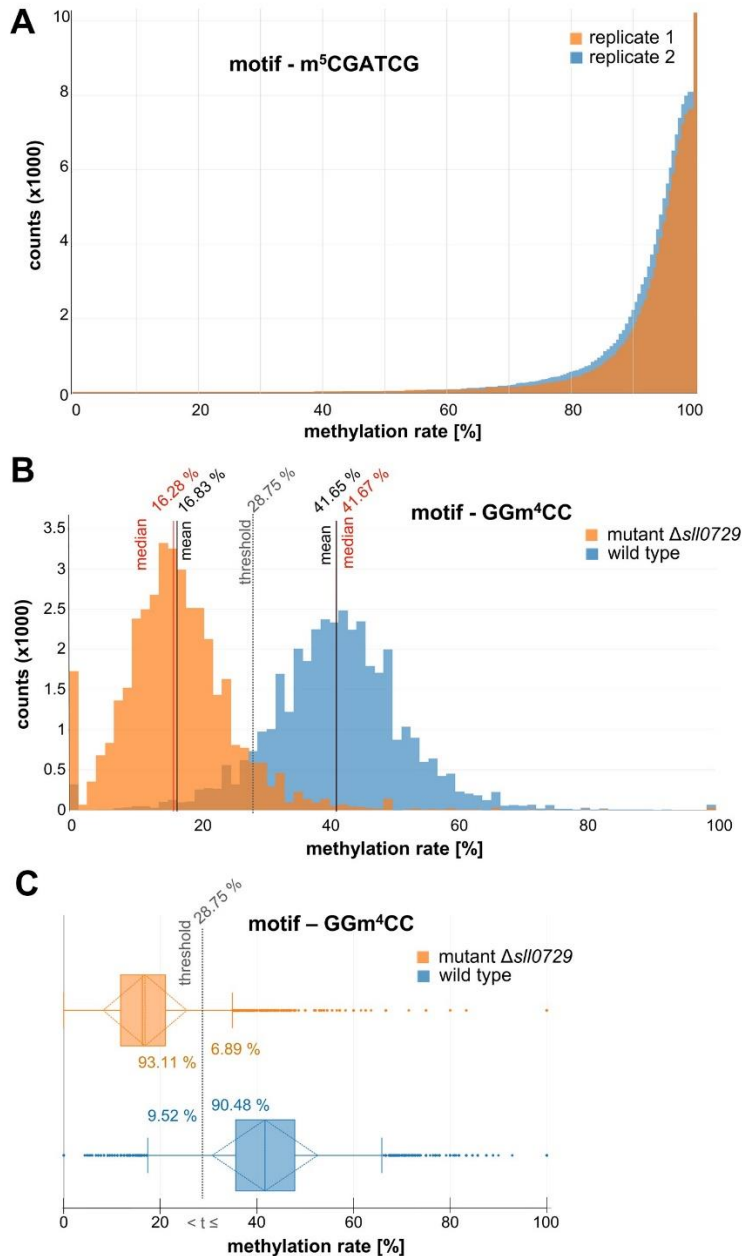
Description	Sequence (5'→3')	amplified ORF or sequence
1803fw	TCCTGAAGGCATGGT	<i>slr1803</i>
1803re	TTGCCATGCTCCATC	<i>slr1803</i>
1803pBADfw	<u>CTCGAGAGTGAAAATTAACA</u>	<i>slr1803</i>
1803pBADre	<u>CTGCAGTCAGCGATGGTAATT</u>	<i>slr1803</i>
0729DELfw	ATGATCTAGCTCCATGGCGA	<i>sll0729</i>
0729DELre	AGGTTATGACGATCCGGCTT	<i>sll0729</i>
0729pBADfw	<u>CTGCAGTTAATAATTTTT</u>	<i>sll0729</i>
0729pBADre	<u>CTG CAG TTA ATA ATT TTT</u>	<i>sll0729</i>
PziaA_XbaI_fw	TAACGAT <u>CTAGAC</u> GTCCATCTCCTTAAT CCGATTCCTG	<i>ziaR</i> + <i>PziaA</i> +5'UTR
PziaA_ClaI_rev	TATCGA <u>ATCGAT</u> CATGGCGGCCAACGT GATTTAAAGAAAAAC	<i>ziaR</i> + <i>PziaA</i> +5'UTR
sll0729_ClaI_fw	TATCGA <u>ATCGAT</u> GAGGAAACCGGGGAA ATAAATAAATCAGC	<i>sll0729</i>
sll0729_XhoI_rev	AATCGA <u>CTCGAG</u> TTAATAATTTTTGATC ATTAACTCTTACCTTTGGAAGC	<i>sll0729</i>
ssl1378_ClaI_fw	TATCGA <u>ATCGAT</u> AGTAATCCTGAAGGT TATAACGTTTGGTCAG	<i>ssl1378</i>
ssl1378_XhoI_rev	AATCGA <u>CTCGAG</u> TTAATTGGACTTTGCC TGGGAATTGGG	<i>ssl1378</i>
slr6095_EcoRI_fw	<u>GAATTC</u> ATGTTATTCCTTAA	<i>slr6095</i>
slr6095_XhoI_rev	<u>CTCGAG</u> CTAAGCCTTTTCCA	<i>slr6095</i>
sll8009_fw	GTTTCATCGCTCCACCTCTC	<i>sll8009</i>
sll8009_rev	TAGGACGGGATACGCTCTTG	<i>sll8009</i>

slr6050_fw	ATATTGAGCAAGTTCGGGGA	<i>slr6050</i>
slr6050_rev	AAACCCCATGCCTACGCCTT	<i>slr6050</i>
slr6050_i_fw	TTAAGTGAGCCTTTGCCTCA	<i>slr6050</i>
slr6050_i_rev	GGTTCTAAAAGGTGTTGATG	<i>slr6050</i>
aphII_fw	ATGAGCCATATTCAACGGGAAACGT	<i>aminoglycoside phosphotransferase II</i>
aphII_rev	TTAGAAAAACTCATCGAGCATCAA	<i>aminoglycoside phosphotransferase II</i>

## Supplementary Figures



**Supplementary Figure S1.** Analysis of the *Synechocystis* methylome by bisulfite sequencing. The snapshot shows the chromosomal section from nt position 2,237,773 to position 2,237,934, which is within gene *slr1938* encoding methylthioribose-1-phosphate isomerase. The bars indicate cytosine methylation on both strands (the bars are displayed on a G for the C at the reverse strand).  $m^5$ CGATCG and GG $m^4$ CC methylations are clearly detectable and highlighted by the red and blue arrows, respectively. The complexity of DNA methylation in *Synechocystis* is highlighted by the region from nt 2,237,865 to 2,237,873, in which six out of nine base pairs are methylated (GGCCGATCG). The 2<sup>nd</sup> and 3<sup>rd</sup> positions in this sequence stretch are methylated by M.Ssp6803II, the 4<sup>th</sup> and 9<sup>th</sup> by M.Ssp6803I, interspersed by methylation on the 6<sup>th</sup> and 7<sup>th</sup> by M.Ssp6803III, which targets G $m^6$ ATC and was detected only by SMRT sequencing (green arrows). Please note that  $m^5$ CGATCG methylation (red arrows) is quantitatively (nearly 100%) displayed by the bisulfite sequencing method, whereas the GG $m^4$ CC methylations (blue arrows) are less sensitive to the bisulfite modifications (around 50%) as shown previously by reference [37].

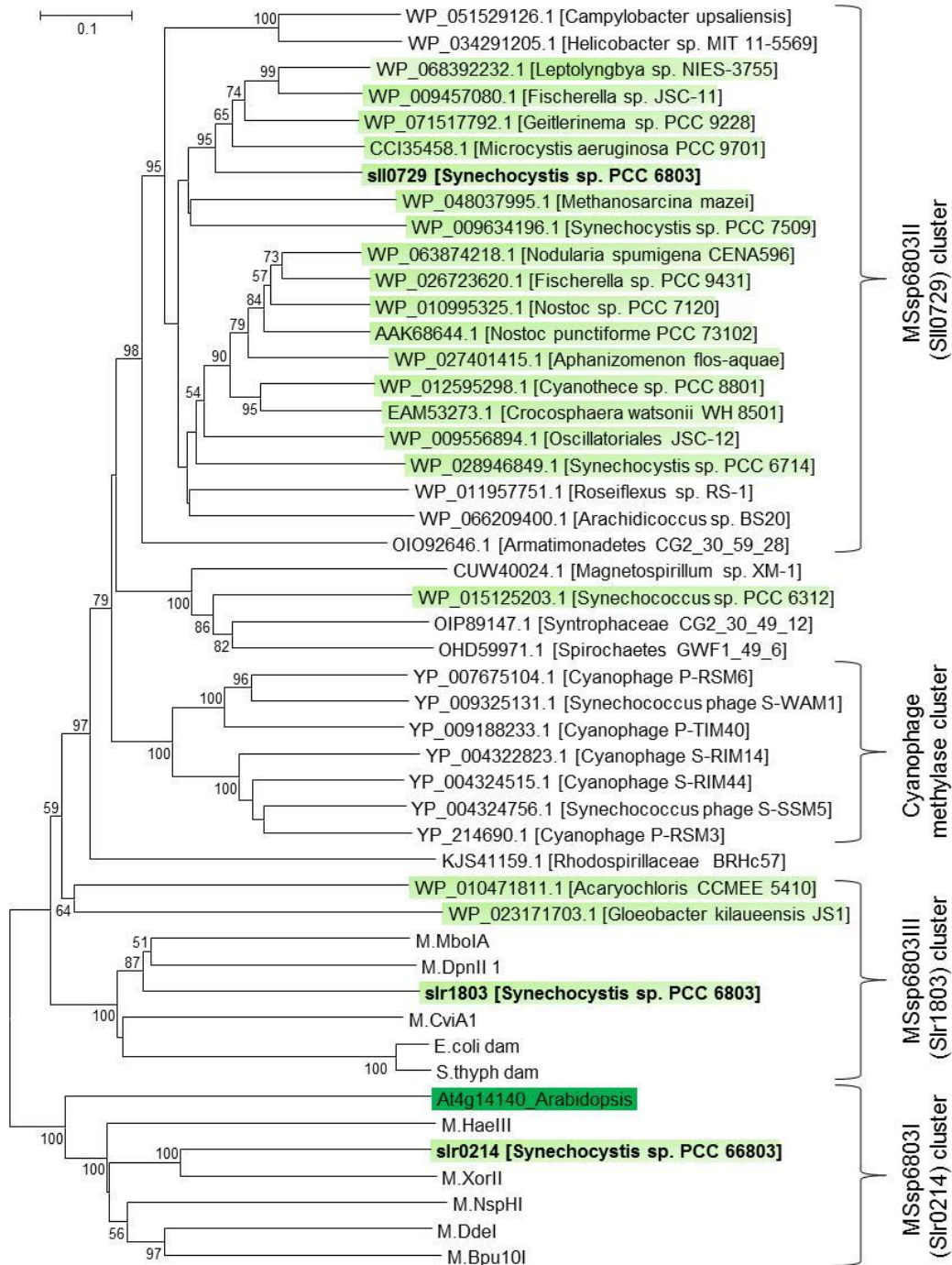


**Supplementary Figure S2. Global analysis of the *Synechocystis* methylome by bisulfite sequencing.**

A. Bisulfite analysis of m<sup>5</sup>CGATCG methylation. There is a total of 38,512 analyzed sites on the chromosome. The cumulative plot shows the percentage of methylation for two replicates. 84.3% (replicate 1, DNA from  $\Delta sll0729$  mutant, orange) and 79.6% (replicate 2 wild-type DNA, blue) of all sites were found to be methylated  $\geq 90\%$ .

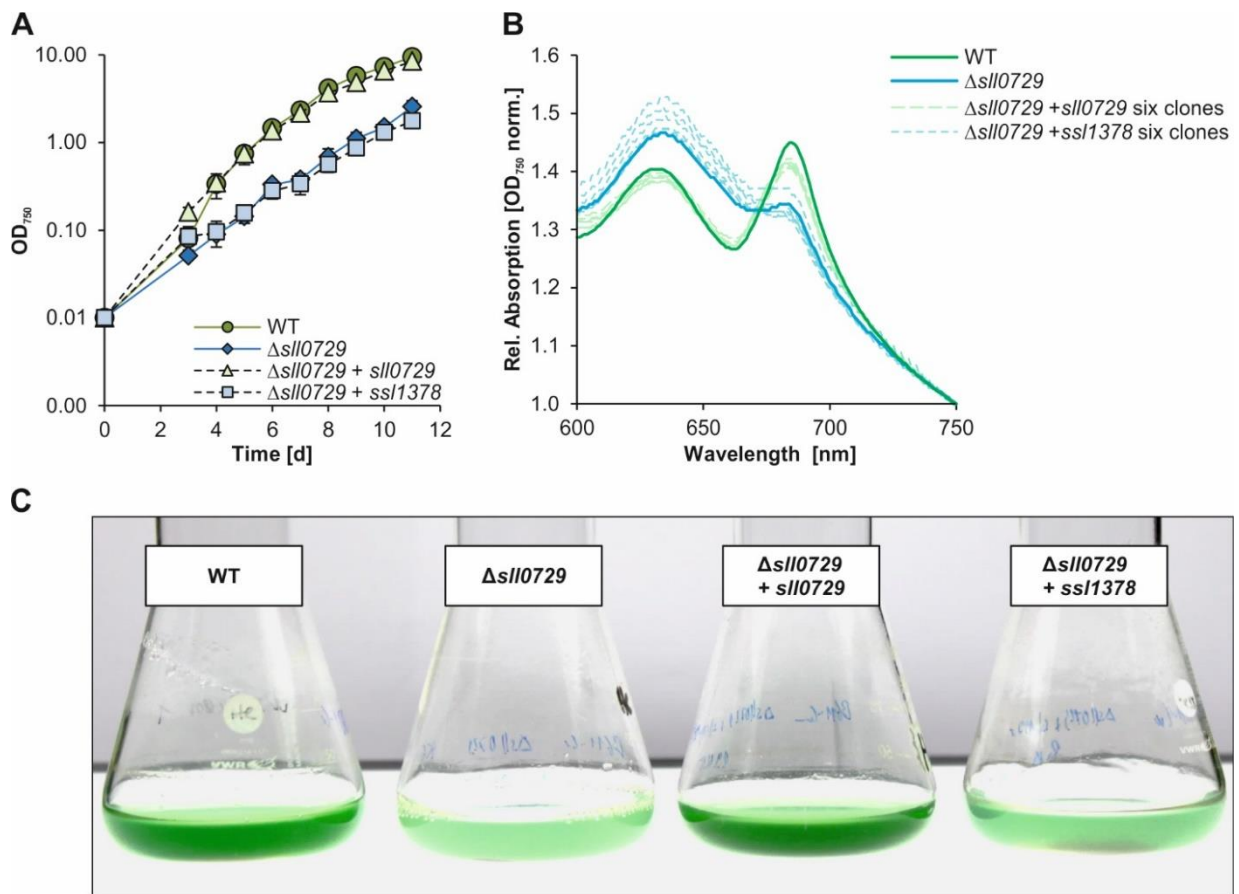
B. Bisulfite analysis of GGm<sup>4</sup>CC methylation. There is a total of 29,852 analyzed sites on the chromosome. The detected percentages of methylation are shown for wild-type DNA (blue) and for the  $\Delta sll0729$  mutant (orange) lacking M.Ssp6803II methylase activity. Because m<sup>4</sup>C is only partially resistant to bisulfite-mediated deamination, an average detected methylation of only 41.65% was detected for the wild type. The 16.83% (mean) detected apparent methylation in the  $\Delta sll0729$  mutant is indicative for the background of the bisulfite conversion rate.

C. Box plot of the bisulfite analysis data of GGm<sup>4</sup>CC methylation from panel B. The local minimum at 28.75% apparent methylation was taken as threshold to separate the two datasets. This classification revealed 90.48% of all sites in the wild type to show methylation and 9.52% to be unmethylated. In contrast, 6.89% of all sites were falsely qualified as methylated in the mutant (false-positives).



**Supplementary Figure S3: Phylogenetic relation of methyltransferases from *Synechocystis* sp. PCC 6803 to related proteins.**

Unrooted neighbor joining tree showing the relation of the characterized DNA-specific methyltransferases (MSsp6803I - Slr0214, MSsp6803II – SII0729, MSsp6803III – Slr1803) to related enzymes found in databases. For the phylogenetic comparison up to 10 of the most similar proteins found in BlastP searches [ref. 32,33] among cyanobacteria (light-green shading) or other bacteria. In addition, functionally characterized methyltransferases were included. Bootstrap values after 1000 replications are indicated when  $\geq 50$ . The evolutionary history was inferred using the Neighbor-Joining algorithm. Evolutionary analyses were conducted in MEGA5 [ref. 35]. Accession numbers of the compared sequences are mentioned in the tree or are as follows: M.DpnII – Acc.No. P04043; M.MboIA – Acc.No. P34720; M.CviA1 – Acc.No. NP\_048937, M.EcoRV – Acc.No. P04393; Dam E.coli – Acc.No. P0AEE9; Dam S.Thyph – Acc.No. P0DMP4; M.XorII – Acc.No. P52311; M.HaeIII – Acc.No. P20589; M.NspHI – Acc.No. AAC97192; M.DdeI – Acc.No. P05302; M.Bpu10I – Acc.No. CAA74996.



**Supplementary Figure S4: Complementation of the  $\Delta sll0729$  phenotype.**

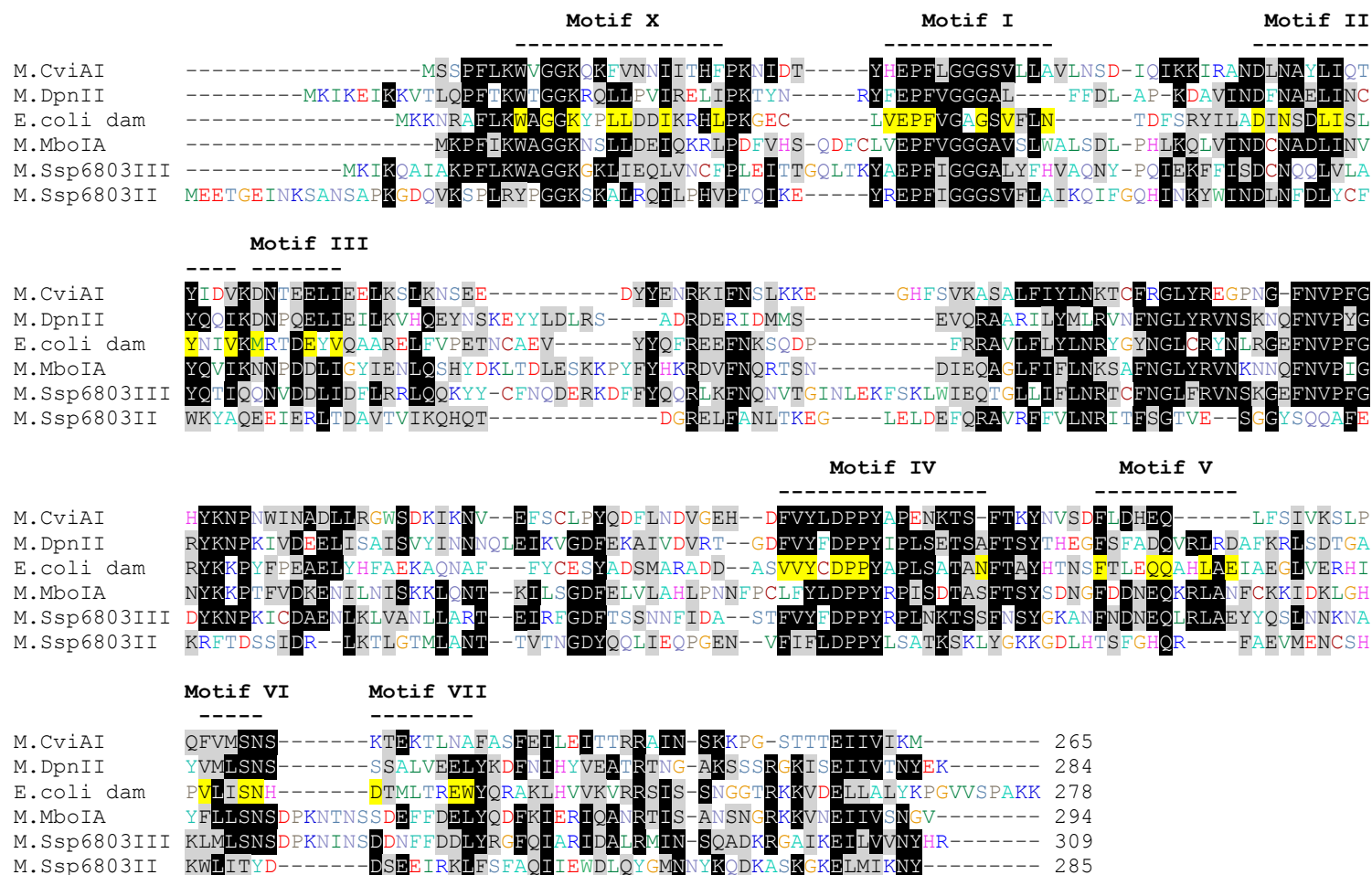
The gene *sll0729* or the downstream located gene *ssl1378* were ectopically expressed in the  $\Delta sll0729$  background driven by the  $Zn^{2+}$ -dependent promoter of the *Synechocystis ziaA* gene.

A: Growth curves for the WT,  $\Delta sll0729$  and the strains harboring a pVZ321-derivative with P*ziaA*-fused *sll0729* or *ssl1378* genes. Cells were cultivated in presence of  $0.77 \mu M Zn^{2+}$ . Data are the mean of 3 biological replicates.

B: Whole cell absorption spectra including six biological replicates (= independent conjugants) for the complementation strains.

C: Photograph of representative cultures after 7 days of growth.





**Supplementary Figure S5: Multiple sequence alignment of characterized adenine-specific methyltransferases as well as the Dam-like protein M.Ssp6803III and the cytosine-specific M.Ssp6803II from *Synechocystis* (second lowest and lowermost rows). Motifs I-VII and X were assigned according to Fig. 1a in Malone et al. [ref. 52] and are indicated. The conserved amino acid residues in the Dam protein of *E. coli* (acc.no. P0AEE9) are highlighted in yellow. Identical amino acid residues are shaded in black and biochemically synonymous amino acid residues in grey. For the corresponding accession numbers see Supplementary Fig. S2.**